Short Communication

First characterization of the surface compounds formed during the reduction of a carbonaceous electrode in LiClO$_4$–ethylene carbonate electrolyte

A. Naji [a], J. Ghanbaja [a], P. Willmann [b], B. Humbert [c], D. Billaud [a]

[a] Laboratoire de Chimie du Solide Minéral, Université Henri Poincaré, Nancy I, BP 239, 54506 Vandoeuvre-les-Nancy Cedex, France
[b] CNES, 18 avenue E. Belin, 31055 Toulouse Cedex, France
[c] CNRS-UHP, LCPE, 54600 Villers-les-Nancy, France

Abstract

Reduction of a carbonaceous electrode in LiClO$_4$–ethylene carbonate electrolyte results in the development of a surface layer formed of Li$_2$CO$_3$ and different lithium alkylcarbonates identified both by electron energy loss and FT-IR spectroscopies.

Keywords: Carbonaceous anodes; Ethylene carbonate; Rechargeable batteries; Lithium perchlorate; Lithium alkylcarbonates; Transmission electron microscopy; Electron energy loss spectroscopy

1. Introduction

'Rocking chair'-type lithium-ion rechargeable batteries operating with lithium–graphite intercalation anodes are now attracting considerable interest [1]. Different types of carbonaceous materials were used as anodes. The concentration of intercalated lithium appeared to be strongly dependent on the nature of the carbon [2,3] and of the composition of the electrolyte [2,4]. In certain conditions, carbons are unstable upon reduction in aprotic electrolytes. For instance, when propylene carbonate (PC) is used as a solvent, graphite exfoliation occurs and lithium intercalation is not observed [5]. In a contrary manner, in selected electrolytes such as LiClO$_4$–ethylene carbonate (EC), reversible intercalation of unsolvated lithium into graphite is possible [3,6]. However, during the first reduction cycle, the intercalation reaction is accompanied by the reduction of the electrolyte and the concomitant deposition of a passivation film on the carbon surface [2,7]. This film, impervious to the solvent molecules allows the reversible lithium intercalation into the graphitic electrode. In this communication, we observed this passivating surface layer using transmission electron microscope techniques (TEM) and Fourier-transform infrared (FT-IR) spectroscopies.

2. Experimental

Transmission electron microscopy (TEM) studies were carried out with a Philips CM 20 Twin Stem apparatus equipped with a parallel detection electron energy loss spectrometer PEELS (Gatan 666). FT-IR spectra were recorded with a Perkin-Elmer 2000 spectrometer.

IR transmission was obtained through a pressed pellet of sample mixed with 3% KCl (w/w).

Characterization by TEM was carried out on composite electrodes composed of 97% (w/w) of natural graphite (UF$_4$, Le Carbone Lorraine) and 3% (w/w) of polyvinylidene fluoride (PVDF) as a binder. The composite electrode made of 97% (w/w) of pitch-based fibers (P 100 Amoco) and 3% (w/w) of PVDF as binder was analysed by FT-IR studies. The BET surface area of UF$_4$ and P 100 fibers are equal to 10 and 76 m^2/g, respectively. Before use, these carbonaceous materials were heated under dynamic vacuum at 430 °C (UF$_4$) and 700 °C (P 100) for several hours.

Electrochemical studies were carried out in a two-electrode cell: (i) the counter-electrode, acting also as a reference electrode, is a lithium ribbon, and (ii) the working electrode is either UF$_4$ or milled P 100 fibers mixed with PVDF. The electrolyte is composed of ethylene carbonate (EC) and

LiClO$_4$ (1.5 mol/kg) outgassed under vacuum at 20 and 150 °C, respectively.

3. Results and discussion

The TEM picture presented in Fig. 1 shows the graphite UF$_4$ surface completely covered with a thin spongy layer. In this case, the graphite electrode was reduced at 0.02 V and reoxidized at 2 V. Analysis of this spongy film by PEELS shows that it contains carbon, oxygen and lithium ion. For a better understanding of the mechanism of the electrolyte decomposition at the carbon surface, analyses were carried out on passivation films formed (i) after a reduction up to 0.8 V (before the beginning of Li$^+$ intercalation) followed by a reoxidation to 2 V and (ii) after a entire charge/discharge cycle between 3 and 0.02 V.

Fig. 2 presents the PEELS spectrum of the UF$_4$–PVDF electrode after a reduction at 0.8 V followed by a reoxidation to 2 V. This spectrum was obtained on particles of the passivation layer isolated in the holes of the amorphous carbon grid of the microscope in order to avoid the superimposition of the spectrum of the sample and that of the amorphous carbon of the grid. The K edge of carbon exhibits two peaks
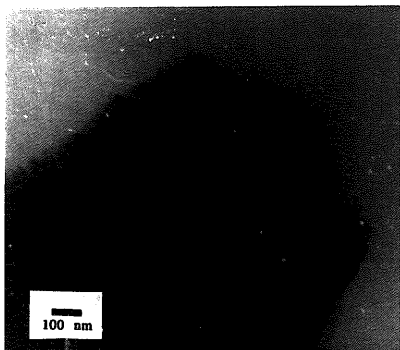

Fig. 1. TEM micrograph of graphite (UF$_4$) after a charge/discharge cycle in EC–LiClO$_4$ at 20 °C.
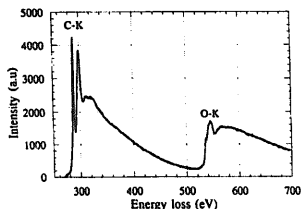

Fig. 2. EELS spectrum of the passivation layer in the case of a graphite electrode reduced at 0.8 V and then reoxidized at 2 V.
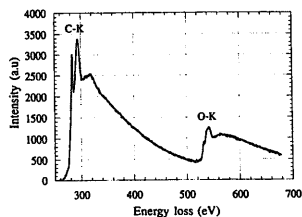

Fig. 3. EELS spectrum of the passivation layer in the case of a graphite electrode reduced at 0.2 V and then reoxidized at 2 V.
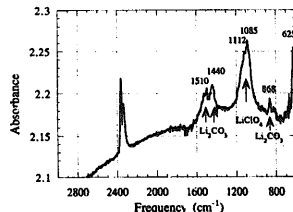

Fig. 4. Transmission FT-IR spectrum of the passivation layer in the case of milled P 100 carbon fibers reduced at 0.8 V and reoxidized at 2 V.

at 289 and 299 eV related respectively to the electronic transitions of the 1s atomic carbon orbitals to the vacant antibonding Π^* and σ^* molecular orbitals corresponding to C=O and C–O groups. The electron energy loss near edge structure (ELNES) of such a passivation film is characteristic of that of a carbonate (O–C=O). Moreover, the quantitative analysis of carbon and oxygen gives an atomic ratio O:C close to 3. Consequently, this spectrum can be attributed to Li$_2$CO$_3$ which was also identified by its characteristic electron diffraction pattern. The EELS spectrum shown in Fig. 3 is obtained when a UF$_4$–PVDF electrode is reduced to 0.2 V and then reoxidized to 2 V. This spectrum is comparable with that presented in Fig. 2. However, the atomic O:C ratio close to 1.5 is characteristic of the lithium alkylcarbonate (–CH$_2$–O–CO$_2$Li)$_2$. Lithium ion is also identified as a component of the passivation film. Other parts of the same passivation films are characterized by O:C ratios close to 1 which gives evidence for the formation of a different alkylcarbonate such as (–CH$_2$–CH$_2$–O–CO$_2$Li)$_2$. Consequently, Li$_2$CO$_3$ is the only species formed at potentials higher than 0.8 V while different lithium alkylcarbonates appear for potentials lower than 0.8 V.

Fig. 4 displays the transmission FT-IR spectrum of the passivation film formed at the surface of a P 100–PVDF electrode reduced at 0.8 V and then reoxidized at 2 V. The three peaks observed at 1510 and 1440 cm^{-1} (ν CO$_3$$^{2-}$) and at 868 cm^{-1} ($\delta$ CO$_3$$^{2-}$) are attributed to Li$_2CO_3$ [8].

In Fig. 5, the FT-IR spectrum obtained by diffuse reflection corresponds to the protective layer formed at the surface of a P 100–PVDF electrode after a complete intensiostatic
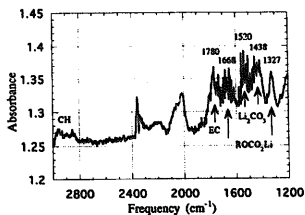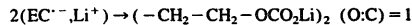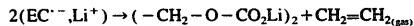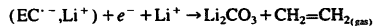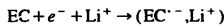
Fig. 5. Diffuse reflection FT-IR spectrum of the passivation layer formed at the surface of P 100 carbon fibers after an intensiostatic charge/discharge cycle.

charge/discharge cycle. In addition to the peaks characteristic for the solvent and the salt $LiClO_4$, other peaks appearing at 1520 and 1438 cm^{-1} are attributed to Li_2CO_3 while those at 1668 cm^{-1} ($\nu_{as}CO_2$) and at 1327 cm^{-1} ($\nu_s CO_2$) are related to lithium alkylcarbonates [7,8].

4. Conclusions

The reduction of EC at the surface of a carbonaceous electrode, in the presence of a lithium salt such as $LiClO_4$, occurs for potentials higher than 0.8 V with the deposition of Li_2CO_3. For potentials lower than 0.8 V, this reduction reaction is continued by the formation of various lithium alkylcarbonates. These different mechanisms are summarized as follows:

$$EC + e^- + Li^+ \rightarrow (EC^{\cdot-}, Li^+)$$

$$(EC^{\cdot-}, Li^+) + e^- + Li^+ \rightarrow Li_2CO_3 + CH_2{=}CH_{2(gas)}$$

$$(O{:}C) = 3$$

$$2(EC^{\cdot-}, Li^+) \rightarrow (-CH_2 - O - CO_2Li)_2 + CH_2{=}CH_{2(gas)}$$

$$(O{:}C) = 1.5$$

$$2(EC^{\cdot-}, Li^+) \rightarrow (-CH_2 - CH_2 - OCO_2Li)_2 \quad (O{:}C) = 1$$

References

[1] S. Megahed and W. Ebner, J. Power Sources, 54 (1995) 155.

[2] R. Fong, U. Von Sacken and J.R. Dahn, J. Electrochem. Soc., 137 (1990) 2009.

[3] D. Billaud, F.X. Henry and P. Willmann, J. Power Sources, 54 (1995) 383.

[4] M. Arakawa and J. Yamaki, J. Electroanal. Chem., 219 (1987) 273.

[5] A.N. Dey and B.P. Sullivan, J. Electrochem. Soc., 117 (1970) 222.

[6] D. Billaud, F.X. Henry and P. Willmann, Mol. Cryst. Liq. Cryst., 245 (1994) 159.

[7] O. Chusid, Y. Ein Ely, D. Aurbach, M. Babai and Y. Carmeli, J. Power Sources, 43–44 (1993) 47.

[8] Y. Ein-Eli, B. Markovsky, D. Aurbach, Y. Carmeli, H. Yamin and S. Luski, Electrochim. Acta, 39 (1994) 2559.